Available online at www.sciencedirect.com
ScienceDirect
Journal of the European Ceramic Society 28 (2008) 493–497
www.elsevier.com/locate/jeurceramsoc

Alkali gallates with mullite-type structure

P. Angerer[a,*], R.X. Fischer[b], M. Schmücker[c], H. Schneider[c]

[a] ECHEM Kompetenzzentrum für angewandte Elektrochemie GmbH, A-2700 Wiener Neustadt, Austria
[b] Fachbereich Geowissenschaften der Universität, D-28359 Bremen, Germany
[c] Deutsches Zentrum für Luft-und Raumfahrt, Institut für Werkstoff-Forschung, D-51147 Köln, Germany

Available online 9 May 2007

Abstract

Silica-free alkali gallates with mullite-type structure were synthesized by reaction of a stoichiometric mixture of the nitrates with glycerol and subsequent thermal treatment between 700 and 900 °C. The crystallization behavior of the compounds has been studied: specimens of the type potassium gallate $K_{0.67}Ga_6^{3+}O_{9.33}$ and rubidium gallate $Rb_{0.67}Ga_6^{3+}O_{9.33}$ have been prepared. The lattice constants (potassium gallate: $a = 8.0065(12)$ Å, $b = 8.0063(10)$ Å, $c = 3.0359(5)$ Å; rubidium gallate: $a = 8.0106(17)$ Å, $b = 8.0161(17)$ Å, $c = 3.0439(6)$ Å) were determined by refinement of the X-ray powder diffraction patterns which show a very close relationship to the alkali aluminate compounds with mullite-type structure. Furthermore isotypes of the composition $Me_{0.67}^{+}(Fe^{3+}, Ga)_6O_{9.33}$ and $Me_{0.67}^{+}(Fe^{3+}, Al)_6O_{9.33}$ (Me^+ = Rb or K) with an Fe(III) content of 20–30% have been prepared.

Keywords: Mullite; Crystal structure; X-ray methods

1. Introduction

The mineral mullite occurs only at a few localities. Synthetic mullite, however, has achieved a great deal of importance in ceramic technology for high temperature applications. The composition of the aluminosilicate phase varies according to $Al_2[Al_{2+2x}Si_{2-2x}]O_{10-x}$. The composition of mullite observed so far ranges between $0.18 \leq x \leq 0.88$ corresponding to 57–92 mol% Al_2O_3.[1] A value of $x = 0$ corresponds to sillimanite, while $x = 1$ can be formally described as pure alumina. The crystal structure of mullite was determined from synthetic solid solution compounds[2,3] and described for 3/2 mullite[4] ($3Al_2O_3{\cdot}2SiO_2$) and for 2/1 mullite[5] ($2Al_2O_3{\cdot}SiO_2$). The Rietveld method was applied to investigate the structural changes as a function of the chemical composition in polycrystalline samples.[6] Only recently, a monograph on the current state of mullite research has been published.[7]

Beside mullite sensu stricto, there exists a family of mullite-type structures characterized by chains consisting of AlO_6-octahedra with common edges. These chains run parallel to the crystallographic *c*-axis and are linked perpendicular to the *c*-axis via (Al, Si)O_4 and AlO_4 tetrahedra grouped to dimers and trimers of two or three tetrahedra linked via a common O-atom.

Several papers have been published on the formation of possible compounds with mullite-type phases in various systems: ι-Al_2O_3[8], Na_2O–Al_2O_3, Na_2O–BaO–Al_2O_3, K_2O–BaO–Al_2O_3,[9] and also $NaAlO_2$–Al_2O_3[10]; furthermore Al_2O_3–B_2O_3, Al_2O_3–Na_2O, and Al_2O_3–K_2O[11] and many other compounds with various compositions belong to the mullite-type family.[7] Additionally to the aluminate phases there are also isotypic germanate compounds.[12] A more detailed structural investigation of the alkali aluminate compounds with mullite-type structure was given more recently.[13,14] The same compounds were investigated by IR-spectroscopy by Voll et al.[15] In case of alkali aluminate phases with mullite structure, the resulting negative charge of the anionic framework $[Al_6O_{10-x}]^{(2-2x)-}$ of the silica-free phase must be compensated by $2-2x$ alkali atoms in the unit cell. Based on crystal chemical considerations confirmed by Rietveld refinements, it has been shown[13] that a stable structure requires exactly a number of 0.67 alkali atoms/unit cell, i.e. each oxygen vacancy is occupied by one alkali atom.

Since the values for the effective ionic radii of Al^{3+} and Ga^{3+} are similar[19,20] (0.53 and 0.61 Å for tetrahedral, and 0.675 and 0.760 Å for octahedral coordination, respectively) and due to the chemical similarity of the two cations it can be expected

* Corresponding author. Tel.: +43 2622 22266 49; fax: +43 2622 22266 50.
E-mail address: paul.angerer@echem.at (P. Angerer).

0955-2219/$ – see front matter © 2007 Elsevier Ltd. All rights reserved.
doi:10.1016/j.jeurceramsoc.2007.03.011

that Al can be substituted by Ga, thus leading to alkali gallate phases with mullite structure. In the present study, we report the preparation and structural characterization of mullite-derived gallates and ferrates.

2. Synthesis procedure

The synthesis of the crystalline compounds was performed according to the same method as suggested by Mazza et al.[11] for the alkali aluminate phases. Initially 10–20 wt.% glycerol (1,2,3-propantriol, $C_3H_8O_3$, Merck no. 1.04092) was added as a reduction agent to a nearly stoichiometric mixture of gallium nitrate hydrate (Aldrich, 22964-4), aluminium nitrate hydrate (Riedel-De Haën no. 31154), or iron(III) nitrate hydrate (Riedel-De Haën no. 31233) with the appropriate anhydrous alkaline nitrates (KNO_3 Merck no. 1.05061, and $RbNO_3$ ABCR no. RB-5147). This mixture was mechanically homogenized and heated with constant stirring. The nitrate mixture starts to decompose at about 110 °C which is indicated by the appearance of reddish-brown NO_2 gas. After this procedure, a spongy amorphous mass is formed. If no further reaction is observed, the sample is transferred in a crucible and calcined in an electric furnace at temperatures between 700 and 900 °C for 4 h to induce the crystallization of the mullite-type phases. At temperatures below this range the crystallization is incomplete and weakly defined diffraction peaks with a large amount of amorphous phase are observed. At temperatures above 900 °C, an increasing amount of corresponding "β-gallate" phases (i.e. $KGa_{11}O_{17}$ International Center of Diffraction Data (ICDD) powder diffraction file PDF 32-0788 or 26-0902, $RbGa_{11}O_{17}$, PDF 26-0933, are recorded.

The synthesis reaction follows the general scheme:

$$2Me^{+}NO_3 + 18Me^{3+}(NO_3)_3{\cdot}9H_2O + 6C_3H_8O_3 + 7O_2$$
$$\Rightarrow 3Me_{0.67}{}^{+}Me_6{}^{3+}O_{9.33} + 56NO_2\uparrow + 18CO_2\uparrow + 186H_2O$$

The highest amounts of mullite-type phase were observed at an atomic ration of alkali/gallium of 1/8, which is not exactly concordant with the ratio in the crystal structure.[13] This is caused by different partition coefficients of the alkali atoms in the crystalline and in the corresponding amorphous phase.

3. Characterization by X-ray powder diffraction

The X-ray powder diffractometry (XRD) method was used for a first characterization of the crystallinity and of the phase composition of the calcined products. The lattice constants of the formed mullite-type phase were subsequently determined.

The average grain size of the material after the calcination process is ≥1 mm. Therefore, the samples were ground to a grain size of about 10 μm in an agate mortar. The measurements were performed with a Siemens D5000 diffractometer (Bragg–Brentano-geometry). This instrument is equipped with a graphite monochromator, automatic divergence slit, and a scintillation counter. Copper Kα radiation (40 kV, 40 mA) was used. The measurements used for the determination of the lattice constants were performed in step-scan mode over the range 14–80° 2θ with a step size of 0.01° and a counting time of 5 s/step. For a first general inspection of the phase composition the step size could be increased up to 0.05° (at 3 s/step).

The program DIFFRAC AT V3.3©Siemens 1993 was applied for the phase identification and the determination of the positions of the diffraction peaks. For the refinement of the cell parameters, the samples were prepared with Silicon powder as an internal standard (2θ values as given in PDF 27-1402, 2nd order correction function of the position correction). These calculations were conducted using the program NBS*AIDS83.[16]

Rietveld refinements of the Rb aluminate and the Rb gallate samples are based on X-ray diffraction data collected with a Philips X'Pert diffractometer with a Ge monochromator in the primary beam yielding a strictly monochromatic radiation. The background was fitted by linear interpolation between reference points set by hand. Intensities within eight times the full width at half maximum of a peak were considered to contribute to the central reflection. Peaks below 50° 2θ were corrected for asymmetry effects using Rietveld's[17] algorithm. The pseudo-Voigt function was used for the simulation of the peak shape, with a refinable parameter defining the Lorentzian and Gaussian character of the peaks as a function of 2θ. The Rietveld analysis[17] was performed using the program suite BRASS, the Bremen Rietveld Analysis and Structure Suite.[18]

4. Results and discussion

Starting from sodium aluminate, potassium aluminate[13,14] and rubidium aluminate phases with mullite-type structure the synthesis experiments were subsequently expanded to gallate compounds. XRD traces of the newly synthesized materials prove clearly the existence of potassium gallate and rubidium gallate phases with mullite-type structure. The XRD traces resemble strongly the corresponding aluminates, however, the peak positions are slightly shifted due to the different unit cell parameters. Sodium gallate or cesium gallate phases, however, could not be synthesized. Solid solution series between rubidium aluminate and rubidium gallate ($Rb_{0.67}(Al_x, Ga_{1-x})_6O_{9.33}$) have been prepared with $x = 0.2$, 0.4, 0.6, 0.8. In this series, a significant enlargement of the unit cell with increasing gallium content is observed. The lattice constant c increases nearly linearly from 2.9420 Å in the pure aluminate compound compared to 3.0439 Å in the pure gallate phase. The relative increase of approximately 3.46% is nearly one order of magnitude higher as in a solid solution series of the type sodium aluminate–potassium aluminate $(Na, K)_{0.67}Al_6O_{9.33}$ in which the alkali cations are substituted. The relative change of the lattice parameters in the rubidium aluminate–rubidium gallate series is nearly the same in each crystallographic direction. On the contrary, the expansion of the unit cell in the sodium aluminate–potassium aluminate series $(Na, K)_{0.67}Al_6O_{9.33}$ differs in each crystallographic direction ($c + 0.47\%$, $a + 0.15\%$, $b - 0.11\%$, relative changes from the sodium to the potassium compound).[13,14] The lattice parameters of the mullite-type compounds in the aluminate–gallate series are displayed in Fig. 1.

It is known that trivalent iron atoms can substitute the aluminum in the alkali β-aluminate phases. As the silica-free

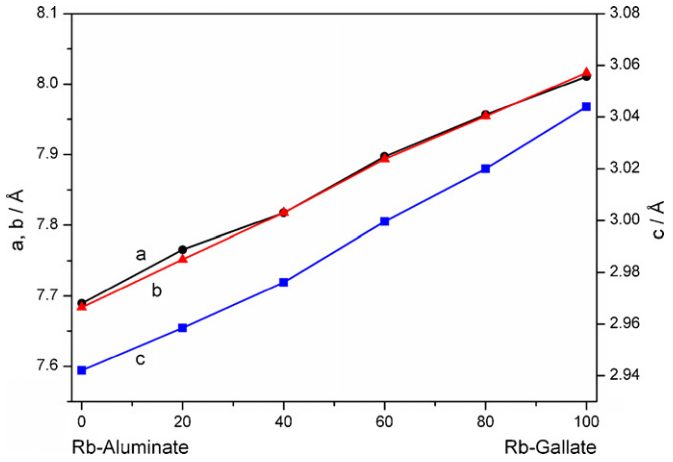

Fig. 1. Lattice constants plotted as a function of the stoichiometric composition within the rubidium aluminate–rubidium gallate binary solid–solution series.

aluminates with mullite-type structure are transforming to the corresponding β-aluminate phases, the synthesis of ferrate(III) phases of the type $Me_{0.67}{}^{+}Fe_6{}^{3+}O_{9.33}$ was also investigated. The synthesis experiments were conducted according to the same method,[11] however, the possibility of the reduction of the iron to the divalent state should be noticed. It turned out that pure alkali ferrate(III) compounds with mullite-type structure could not be achieved but significant substitution of Al^{3+} and Ga^{3+} by Fe^{3+} is possible in rubidium aluminate and in rubidium gallate compounds. Starting from the pure aluminate or gallate phase a linear shift of the diffraction peaks of the mullite-type phase with increasing Fe(III) content can be observed. In Fig. 2, the lattice constants of these compounds are displayed as a function of the iron content in the starting mixture. It should be noted that the iron content in the starting mixture need not be equivalent to the content in the crystalline phase. However, the nearly linear graph indicates an equilibrated incorporation of the trivalent iron in the mullite-type phase. The diffraction intensities of the mullite-type phases are decreasing with rising iron content. Above a maximum Fe(III) content of 30% in the gallate series

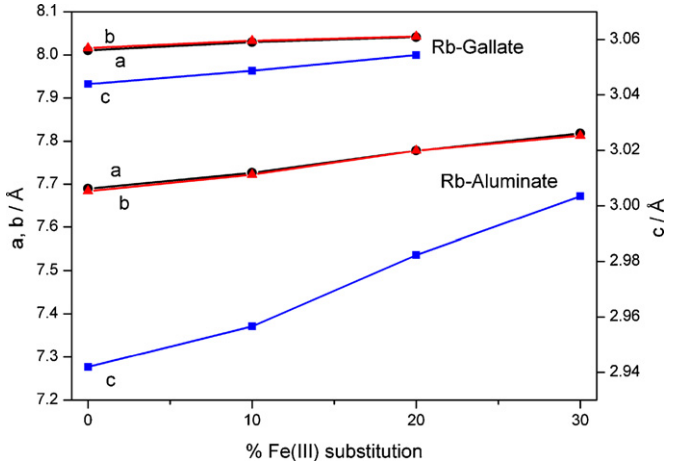

Fig. 2. Lattice constants plotted as a function of the Fe(III) substitution for aluminium or gallium in the rubidium aluminate and in the rubidium gallate compound.

Table 1
Lattice constants of alkali aluminates and gallates calculated in Rietveld refinements

Compound	*a* (Å)	*b* (Å)	*c* (Å)	Void space (Å)	Reference
$Na_{0.67}Al_6O_{9.33}$	7.6819(4)	7.6810(4)	2.91842(8)		10
$K_{0.67}Al_6O_{9.33}$	7.6934(3)	7.6727(3)	2.93231(7)	2.87	10
$Rb_{0.67}Al_6O_{9.33}$	7.6905(5)	7.6807(5)	2.9420(1)	2.90	this work
$Rb_{0.67}Ga_6O_{9.33}$	8.0087(3)	8.0177(3)	3.04158(6)	2.98	this work

Void space calculated as mean value of the six closest distances from the center to the next oxygen neighbors.

and of 40% in the aluminate series no such phases are observed, the corresponding samples consisting mainly of weakly crystallized γ-Al_2O_3 and γ-Ga_2O_3 phases with large amounts of coexisting amorphous phase. An extrapolation of the determined lattice constants suggests a hypothetical rubidium ferrate(III) with mullite-type structure with $a = 8.2$ Å, $b = 8.2$ Å, $c = 3.1$ Å.

The X-ray diffraction patterns of the rubidium aluminate and the rubidium gallate samples conform to the unit cell parameters of mullite in space group *Pbam* within the tolerance expected for the chemical substituents. However, the intensities differ significantly from the alkali mullites studied previously.[13] The Rb aluminate is poorly crystalline with a high amount of amorphous components and γ-Al_2O_3 as impurity. The poor quality of this sample and its X-ray diffraction data did not allow a detailed analysis of the crystal structure. However, Rietveld refinement with starting parameters from the potassium aluminate of our previous alkali aluminate work confirmed the basic structural features of the alkali aluminates with mullite-type structure, with the chains of edge sharing octahedra parallel *c* and the bridging triclusters of aluminate tetrahedra. Rb resides in the voids of the oxygen vacancies at 0, 1/2, 1/2 similarly to Na and K in the other alkali aluminates. The Rb position has a distance of less than 1 Å to the Oc* atom which causes high correlations between their positional and thermal parameters. Calculated and observed intensities showed a reasonably good fit sufficient for the determination of the lattice parameters which are given in Table 1.

The X-ray diffraction data of the rubidium gallate sample have a much better signal to noise ratio and higher absolute intensities than the corresponding aluminate data which reduced the correlation problems between the partially occupied Rb and Oc* sites. Several peaks in the diffraction pattern indicate an impurity phase identified as a rubidium gallium carbonate hydrate. Although, its crystal structure has not been determined yet and its unit cell parameters given in the powder diffraction file (PDF 26-1366) of the International Center of Diffraction Data (ICDD) are obviously wrong, all impurity reflections observed in the Rb gallate diagram perfectly match the data in the PDF. Fortunately, there are essentially no overlapping peaks, and consequently, the impurity effects can be excluded without affecting the refinements.

Different Fourier analyses immediately revealed that the Rb atoms reside on or close to the 2(d) site[21] in 0, 1/2, 1/2. Placing the Rb atom in the special position resulted in a rather high displacement factor of $B = 2.4$ Å^2 for Rb and a negative parameter $B = -2.0$ Å^2 for Oc*. Shifting the Rb atom off the special

Table 2
Positional parameters, isotropic displacement factors (Å^2), site symmetry, Wyckoff position, and occupancies of the mullite-type rubidium gallate

Atom	*X*	*Y*	*Z*	*B* (Å^2)	Site symmetry	Wyckoff position	No. of atoms/unit cell
Rb	0.473(2)	0.019(2)	1/2	0.6(2)	... *m*	4h	0.67
M1(Ga)	0	0	0	0.68(4)	... 2/*m*	2a	2
T(Ga)	0.1574(4)	0.3304(4)	1/2	1.14(5)	... *m*	4h	2.67
T*(Ga)	0.2757(6)	0.1969(7)	1/2	0.9(1)	... *m*	4h	1.33
O1	0.3571(8)	0.4211(8)	1/2	0.7(1)	... *m*	4h	4
O2	0.1321(10)	0.2051(8)	0	1.1(2)	... *m*	4g	4
O4	0.420(4)	0.069(5)	1/2	0.1(5)	... *m*	4h	1.33

Note: data for site symmetry and Wyckoff position taken from International Tables of Crystallography.[21]

Table 3
Selected interatomic distances (Å) of the mullite-type rubidium gallate

Rb–O1	2.76(2)	2 × M1–O2	1.956(7)	T–O1	1.757(7)	T*–O4	1.54(4)
2 × Rb–O2	2.97(2)	4 × M1–O1	2.006(4)	2 × T–O2	1.834(4)	2 × T*–O2	1.908(6)
2 × Rb–O2	3.06(2)			T–O4	2.01(4)	T*–O1	1.912(9)
2 × Rb–O1	3.11(2)						
Mean	3.01		1.989		1.859		1.817

position yielded *B* values of 0.7 and 0.1 Å^2 for Rb and Oc*, respectively. The Bragg residual, which is the most significant measure for the changes in the crystal structures, dropped from 6.5 to 5.9% which represents the final status of the refinements. Structural data (atomic positions, displacement factors, site symmetry, Wyckoff positions and occupancies) are listed in Table 2, selected interatomic distances and angles are given in Table 3. The fit between observed and calculated intensities of the X-ray diffraction data of the Rb gallate is shown in Fig. 3.

The thermal parameter for Oc* is still slightly too small which might reflect the still existing high correlations between the parameters of these two atoms (Oc* and Rb). The offset from the special position does not follow the sequence of the sodium and potassium aluminates previously studied,[13] where the smaller Na atom was in the split position and the bigger K atom was determined to reside in the special position. The rubidium atom with an effective ionic radius of 1.52 Å is even bigger than the K atom (1.38 Å) and nevertheless is shifted towards the oxygen atoms of the octahedron. Here it should be noted that the octahedral and tetrahedral sites are occupied by gallium atoms which significantly expands the coordination polyhedra and consequently also expands the void space between them. This is also expressed by the expanded lattice constants as compared with the other alkali mullite-type compounds (cf. Table 1).

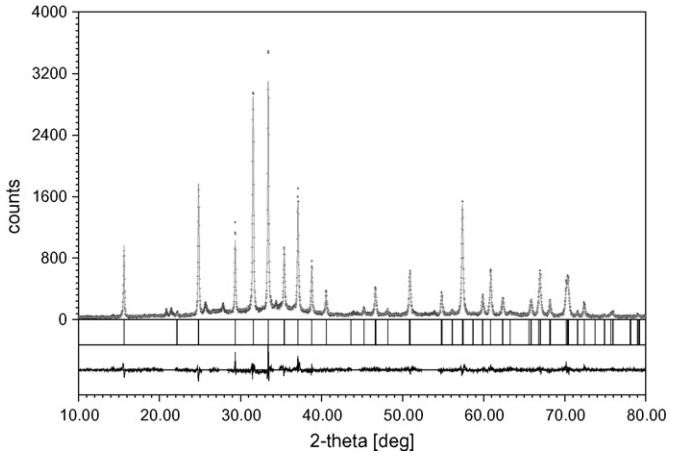

Fig. 3. Observed (crosses) and calculated (solid line) powder patterns of mullite-type rubidium gallate with difference curves underneath. Peak positions permitted by the cell parameter are indicated by tick marks. Impurity peaks belong to a rubidium gallium carbonate hydrate.

5. Conclusion

This work continues the previous synthesis experiments of the alkali aluminate compounds. Here a sodium aluminate, potassium aluminate and rubidium aluminate with mullite-type structure has been found. Between these phases, a continuous miscibility was observed. No isotypic cesium aluminate has been observed. In the gallate system, only potassium and rubidium phases with mullite-type structure could be identified. The ratio of the ionic radius of the alkali cation relative to the corresponding value of the trivalent atom in the octahedral and tetrahedral anionic framework is crucial. No cesium gallate with mullite-type structure could be prepared. In this case, most likely cesium phases of higher stability inhibit the formation.

The substitution of Ga(III) by Fe(III) in the anionic framework must be discussed separately. Here the effect on the shift of the lattice parameters is higher. The ionic radius of Fe^{3+} is closer to the value of Ga^{3+} than to corresponding values of Al^{3+}. However, the limit of the Fe(III) substitution in the rubidium aluminium compound (30 mol%) is higher than in the rubidium gallate (20 mol%).

Acknowledgement

This work was supported by the Deutsche Forschungsgemeinschaft (DFG SFB 408 “Anorganische Festkörper ohne Translationssymmetrie”).

References

1. Fischer, R. X., Schneider, H. and Voll, D., Formation of aluminum rich 9:1 mullite and its transformation to low alumina mullite upon heating. *J. Eur. Ceram. Soc.*, 1996, **16**, 109–113.
2. Ďurovič, S., A statistical model of the crystal structure of mullite. *Kristallografiya*, 1962, **7**, 339–349.
3. Sadanaga, R., Tokonami, M. and Takeuchi, Y., The structure of mullite, $2Al_2O_3{\cdot}SiO_2$, and relationship with the structures of sillimanite and andalusite. *Acta Crystallogr.*, 1962, **15**, 65–68.
4. Saalfeld, H. and Guse, W., Structure refinement of 3: 2 mullite ($3Al_2O_3{\cdot}2SiO_2$). *N. Jb. Miner. Mh.*, 1981, **4**, 145–150.
5. Angel, R. J. and Prewitt, C. T., Crystal structure of mullite: a re-examination of the average structure. *Am. Mineral.*, 1986, **71**, 1476–1482.
6. Ban, T. and Okada, K., Structure refinement of mullite by the Rietveld method and a new method for estimation of chemical composition. *J. Am. Ceram. Soc.*, 1992, **75**, 227–230.
7. Schneider, H. and Komarneni, S., ed., *Mullite*. Wiley, VCH, Weinheim, 2005.
8. Foster, P. A., Nature of alumina in quenched cryolite-alumina melts. *J. Electrochem. Soc.*, 1959, **106**, 971–975.
9. Perrotta, A. J. and Young, J. E., Silica-free phases with mullite-type structures. *J. Am. Ceram. Soc.*, 1974, **57**, 405–407.
10. Elliot, A. G. and Huggins, R. A., Phases in the system $NaAlO_2$–Al_2O_3. *J. Am. Ceram. Soc.*, 1975, **58**, 497–500.
11. Mazza, D., Vallino, M. and Busca, G., Mullite-type structures in the systems Al_2O_3–Me_2O (Me = Na, K) and Al_2O_3–B_2O_3. *J. Am. Ceram. Soc.*, 1992, **75**, 1929–1934.
12. Gelsdorf, G., Müller-Hesse, H. and Schwiete, H. E., Einlagerungsversuche an synthetischem Mullit und Substitutionsversuche mit Galliumoxyd und Germaniumoxyd. Teil II. *Arch. Eisenhüttenwesen*, 1958, **29**, 513–519.
13. Fischer, R. X., Schmücker, M., Angerer, P. and Schneider, H., Crystal structures of Na and K aluminate mullites. *Am. Mineral.*, 2001, **86**, 1513–1518.
14. Angerer, P., *Alkalialuminate und Alkaligallate mit Mullitstruktur*, Ph.D. Thesis, University of Hannover, 2001.
15. Voll, D., Angerer, P., Beran, A. and Schneider, H., A new assignment of IR vibrational modes in mullite. *Vibr. Spectrosc.*, 2002, **30**, 237–243.
16. Mighell, A.D., Hubbard, C.R. and Stalick, J.K., NBS*AIDS83. A FORTRAN program for crystallographic data evaluation. NBS Technical Note 1141, 1983.
17. Rietveld, H. M., A profile refinement method for nuclear and magnetic structures. *J. Appl. Crystallogr.*, 1969, **2**, 65–71.
18. Birkenstock, J., Fischer, R. X. and Messner, T., BRASS, the Bremen Rietveld Analysis and Structure Suite. *Z. Krist. Suppl.*, 2006, **23**, 237–242.
19. Shannon, R. D. and Prewitt, C. T., Effective ionic radii in oxides and fluorides. *Acta Cryst.*, 1969, **B25**, 925–946.
20. Shannon, R. D., Revised effective ionic radii and systematic studies of interatomic distances in halides and chalcogenides. *Acta Cryst.*, 1976, **A32**, 751–767.
21. Hahn, T. ed., *International Tables for Crystallography*, *Vol. A*. Kluwer Academic Publishers, Dordrecht, Boston, London, 2002.